

UNCLASSIFIED

AD NUMBER

AD294138

LIMITATION CHANGES

TO:

Approved for public release; distribution is unlimited.

FROM:

Distribution authorized to U.S. Gov't. agencies and their contractors;
Administrative/Operational Use; JAN 1963. Other requests shall be referred to Air Force Arnold Engineering Development Center, Arnold AFB, TN.

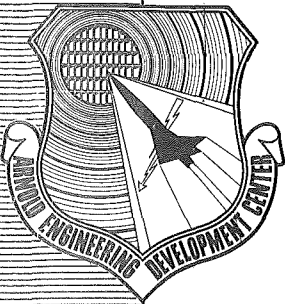
AUTHORITY

aedc per dtic form 55

THIS PAGE IS UNCLASSIFIED

AEDC-TDR-62-196

RTF RESEARCH BRANCH



**ZERO SECONDARY FLOW
EJECTOR-DIFFUSER PERFORMANCE
USING ANNULAR NOZZLES**

By

**R. C. German, J. H. Panesci, and H. K. Clark
Rocket Test Facility
ARO, Inc.**

TECHNICAL DOCUMENTARY REPORT NO. AEDC-TDR-62-196

January 1963

AFSC Program Area 750G, Project 6950, Task 695002

**(Prepared under Contract No. AF 40(600)-1000 by ARO, Inc.,
contract operator of AEDC, Arnold Air Force Station, Tenn.)**

**ARNOLD ENGINEERING DEVELOPMENT CENTER
AIR FORCE SYSTEMS COMMAND
UNITED STATES AIR FORCE**

NOTICES

Qualified requesters may obtain copies of this report from ASTIA. Orders will be expedited if placed through the librarian or other staff member designated to request and receive documents from ASTIA.

When Government drawings, specifications or other data are used for any purpose other than in connection with a definitely related Government procurement operation, the United States Government thereby incurs no responsibility nor any obligation whatsoever; and the fact that the Government may have formulated, furnished, or in any way supplied the said drawings, specifications, or other data, is not to be regarded by implication or otherwise as in any manner licensing the holder or any other person or corporation, or conveying any rights or permission to manufacture, use, or sell any patented invention that may in any way be related thereto.

ZERO SECONDARY FLOW
EJECTOR-DIFFUSER PERFORMANCE
USING ANNULAR NOZZLES

By

R. C. German, J. H. Panesci, and H. K. Clark

Rocket Test Facility

ARO, Inc.

a subsidiary of Sverdrup and Parcel, Inc.

January 1963

ARO Project No. RW2141


ABSTRACT

An investigation was conducted to determine the performance of zero-secondary flow ejector-diffuser systems using annular driving nozzles. Eight annular nozzles with various geometries, including one expansion-deflection (E-D) nozzle were tested in cylindrical diffusers having various diffuser lengths. The ejector starting and pumping characteristics were compared and found similar to the empirical relations developed for ejectors having conventional convergent-divergent nozzles. The unique problems associated with simulated altitude testing of the E-D nozzle and the effects of ejector-diffuser design on E-D nozzle performance are discussed. A method is described for determining the ejector pumping characteristics when the ejector is unstarted to satisfy the annular nozzle test requirement for altitude simulation at conditions other than minimum cell pressure.

PUBLICATION REVIEW

This report has been reviewed and publication is approved.


Donald R. Eastman, Jr.
DCS/Research


Jean A. Jack
Colonel, USAF
DCS/Test

CONTENTS

	<u>Page</u>
ABSTRACT.	iii
NOMENCLATURE.	vii
1.0 INTRODUCTION	1
2.0 DISCUSSION OF EJECTOR-DIFFUSER PROBLEMS ASSOCIATED WITH ANNULAR NOZZLES.	1
3.0 EXPERIMENTAL STUDY	4
4.0 DISCUSSION OF EXPERIMENTAL RESULTS	6
5.0 CONCLUSIONS	13
REFERENCES	14

TABLES

1. Description of Ejector-Diffuser Test Configurations . .	17
2. Description of Annular Nozzles	18
3. Description of Measuring Instruments	19

ILLUSTRATIONS

Figure

1. Types of Annular Nozzles	21
2. Typical Operation of an Expansion-Deflection Nozzle in an Ejector-Diffuser System.	22
3. Typical Ejector-Diffuser Test Configuration.	23
4. Annular Nozzle Configurations Tested	24
5. Typical Total Pressure Rake Installation	25
6. Typical Ejector Starting Phenomenon for Constant Nozzle Total Pressure	26
7. Effect of Diffuser Length on Ejector Starting and Operating Pressure Ratio for Various Annular Nozzles	27

<u>Figure</u>	<u>Page</u>
8. Effect of Diffuser Length on Ejector Starting Characteristics	
a. S1-P1-10 Ejector Configuration.	28
b. S3-P1-10 Ejector Configuration.	29
9. Comparison of the Starting Pressure Ratio Correction Factor for Various Annular Nozzle Configurations with That Obtained for C-D Nozzles	30
10. Correction to Normal Shock Pressure Ratio Required for Various Diffuser Length Ratios	30
11. Effect of Reynolds Number on Minimum Cell Pressure Ratio	31
12. Comparison of the Ratio of Experimental and Calculated Minimum Cell Pressure Ratio for Various Annular Nozzle Configurations with That Obtained for C-D Nozzles.	32
13. Graphical Solution for Subsonic Mach Number at Station Two	33
14. Comparison of Theoretical and Experimental Ejector Pumping Characteristics for Various Annular Nozzle Configurations; $(L/D)_d = 9.0$, $p_t = 45$ psia	
a. Configurations S1-P2-10, S1-P3-10, S2-P2-10, S3-P1-10, and S3-P1-6	34
b. Configurations S4-P1-10 and E-D-6	35
15. Effect of Diffuser Diameter on E-D Nozzle Wall Static Pressure Distribution	36
16. Effect of Second Throat on E-D Nozzle Wall Static Pressure Distribution, $D_d = 6.12$ in.	37
17. Mach Number Distribution Downstream of E-D Nozzle for Various Cell Pressure Ratios ($D_d = 10.19$ in., $p_t = 40$ psia)	38

NOMENCLATURE

A	Cross-sectional area
D	Diameter
F	Total force
K	Correction factor (see Eq. 1)
K'	Correction factor (see Eq. 2)
L	Length
ℓ	Distance between nozzle shroud exit and nozzle spike tip
M	Mach number
m	Mass flow
p	Static pressure
p_r	Rake pressure (static and/or total)
p_t	Nozzle total pressure
R	Gas constant
R_{ne}	Reynolds number based on nozzle exit flow conditions
T	Static temperature
T_t	Total temperature
X_p	Distance between nozzle throat and nozzle spike tip
X_r	Distance between nozzle shroud exit and total pressure rake
γ	Ratio of specific heats
θ_{ne}	Nozzle shroud divergence angle at nozzle exit
θ_p	Nozzle plug half angle
θ^*	Nozzle throat angle
θ_{st}	Second throat inlet angle

SUBSCRIPTS

b	Plug base
c	Ejector cell

calc	Calculated
d	Cylindrical diffuser
eff	Effective
exper	Experimental
ex	Exhaust
j	Jet flow field at station (1)
min	Minimum
n	Nozzle
ne	Nozzle exit
ns	Normal shock
oper	Operate
p	Nozzle plug or spike
Pe	Station on nozzle spike corresponding to nozzle shroud exit
r	Rake
s	Nozzle shroud
st	Second throat
start	Start
1, 2	Station numbers

SUPERSCRIPT

*	Nozzle throat
---	---------------

1.0 INTRODUCTION

Considerable knowledge has been gained at the Rocket Test Facility (RTF), Arnold Engineering Development Center (AEDC), Air Force Systems Command (AFSC), concerning the design of ejector systems without induced flow which use the energy of the exhaust gas to reduce the pressure in the test cell. The ejector research programs to date have included the effect of the following parameters on ejector-diffuser performance using conventional convergent-divergent driving nozzles:

1. Effect of nozzle area ratio and diffuser diameter (Ref. 1).
2. Effect of conical inlets (Ref. 2).
3. Effect of diffuser length (Ref. 3).
4. Effect of Reynolds number (Ref. 4).
5. Effect of second throat geometry (Ref. 5).

Because it was not known whether the results of these investigations could be applied to ejector systems using annular nozzles, a study was initiated at RTF during the period April 1, 1961, to June 1, 1962, to determine the effect on ejector performance of various annular nozzle configurations as well as to determine the influence of several ejector configurations on nozzle performance. Eight annular nozzles having various geometries including an expansion-deflection nozzle were tested to determine their effect on ejector starting and operating and on ejector pumping (minimum cell pressure) characteristics. The effects of diffuser length and of varying Reynolds number on these characteristics were also investigated. These results are compared with the ejector-diffuser performance obtained with the more conventional convergent-divergent nozzles and indicate that existing methods may be used to estimate the ejector performance for annular nozzles.

2.0 DISCUSSION OF EJECTOR-DIFFUSER PROBLEMS ASSOCIATED WITH ANNULAR NOZZLES

The application of the annular type nozzle as a rocket propulsion element has been intensively investigated by several major rocket motor manufacturers because of the performance increase of certain

Manuscript released for printing January 1963.

annular nozzle designs above that of a conventional convergent-divergent nozzle (herein called C-D nozzle) in the overexpanded condition ($p_{ne} < p_c$) and because of its apparent advantage in size, weight, and thrust vectoring capabilities (Ref. 6).

Simulated altitude testing of these annular-throated rocket nozzles present problems in the design of an ejector-diffuser system which have not been encountered during tests with C-D nozzles.

2.1 TYPES OF ANNULAR NOZZLES

An investigation of the method of supersonic expansion of the exhaust gases suggests that annular-throated nozzles may be divided into two major groups:

1. The nozzles in which the expansion process is directly or indirectly regulated by the ambient pressure with a minimum amount of losses when compared to an ideal expansion. These "self-adjusting" type nozzles can be further divided into two categories
 - a. The nozzles in which the exhaust jet adjusts to ambient pressure by altering the outer boundary of the jet, such as the spike nozzle (Fig. 1a).
 - b. The nozzle which allows the exhaust jet to adjust to high ambient pressures by altering the size of the central subsonic core downstream of the nozzle plug, such as the expansion-deflection (herein called E-D) type nozzles (Fig. 1b).
2. The nozzles in which the expansion of the exhaust gases to high ambient pressures is accomplished only by separation resulting in significant losses, such as the non-self adjusting shrouded-spike nozzle (Fig. 1c).

In this report a spike nozzle will refer to an annular nozzle whose centerbody converges to a point, and a plug nozzle will refer to an annular nozzle containing a blunt centerbody, with the exception of the E-D nozzle which will be referred to by name.

2.2 EJECTOR-DIFFUSER DESIGN PROBLEMS

Considerable information has been gained in previous investigations regarding ejector-diffuser performance using C-D type nozzles; however, it was not known whether this information was applicable for annular-type nozzles. A qualitative analysis was therefore made

of the ejector-diffuser problems associated with each type of annular nozzle.

2.2.1 Nozzles with No Self-Adjustment

In this type of nozzle (Fig. 1c) the exhaust gases are made to expand in a diverging annulus formed between the converging central spike and the diverging shroud. The ejector pumping characteristics for this type nozzle were expected to be similar to those for a C-D nozzle having the same area ratio, A_d/A^* ; however, the influence of the central spike on the ejector starting characteristics was unknown.

2.2.2 Nozzles with External Self-Adjustment

The exhaust gases from a spike nozzle with external self-adjustment (Fig. 1a) are controlled by the ambient pressure in which the nozzle is operating and by the spike surface. The effective nozzle area ratio therefore varies because of the self-adjusting characteristics of the nozzle exhaust gas with changes in ambient pressure. The effect of this varying nozzle boundary on ejector starting and pumping characteristics was unknown. This self-adjusting feature also poses an additional problem because of the test requirement for altitude simulation at conditions other than minimum cell pressure. One method of increasing the cell pressure would be to operate the ejector unstated* by increasing the exhaust pressure. Thus, it is desirable to determine the relationship between exhaust pressure and cell pressure when the ejector is unstated. As with the shrouded spike nozzle discussed in section 2.2.1, the influence of the nozzle spike on the ejector starting characteristics was also unknown.

2.2.3 Nozzles with Internal Self-Adjustment

The ejector operation of nozzles having separation behind a central plug, such as the E-D nozzle, can be divided into three distinct flow regimes (see Fig. 2):

1. Ejector unstated; plug wake open.
2. Ejector unstated; plug wake closed.
3. Ejector started; plug wake closed.

The first regime results when the static pressure of the exhaust gas is equal to ambient pressure and a core of subsonic gas exists in

*See section 4.1.

the center of the nozzle. Simulated altitude testing at these conditions presents a problem in that a disturbance to the rocket exhaust flow field external to the rocket nozzle may feed back through the subsonic core into the nozzle and thus affect nozzle performance.

As the ambient pressure is decreased, the high energy exhaust gases decrease the plug base pressure in the subsonic core causing the wake behind the nozzle plug to close. This results in the second regime with a constant and minimum plug base pressure. The closing action of the wake results in an increase in the effective nozzle area ratio such that the nozzle flow is overexpanded during the initial portion of this regime.

The third regime of operation occurs when the nozzle is under-expanded such that the free jet expands downstream of the nozzle, resulting in the ejector becoming started. Ejector design for simulated altitude testing at these conditions may be considered similar to the ejector design for a conventional underexpanded C-D nozzle in which the ejector is started.

3.0 EXPERIMENTAL STUDY

3.1 EXPERIMENTAL APPARATUS

Twenty-six ejector configurations (Table 1) were tested by combining eight annular nozzle configurations (Table 2) with two straight cylindrical diffusers of various lengths and one second throat. The nozzles were concentrically located in the diffusers with the upstream end of the diffuser attached to a sealed plenum chamber. A typical test configuration is shown in Fig. 3.

3.1.1 Nozzle Design

The annular supersonic nozzles that were tested included an expansion deflection nozzle and a basic annular nozzle configuration which was designed such that various nozzle geometries and area ratios were possible by exchanging the four shroud and three nozzle centerbody combinations. Dimensional details of these nozzles are presented in Table 1, and the nozzle configurations are shown in Fig. 4. All of the nozzles were fabricated from brass and the mating surfaces of all the nozzle components were provided with "O"-ring seals. Static pressure taps were located in a spiral arrangement along the nozzle wall and plug surface.

3.1.2 Test Cell Description

Most of the testing was accomplished with two cylindrical diffusers. One had an inside diameter of 10.19 in. with length to diameter ratios of approximately $(L/D)_d = 9, 6,$ and 3 , and the second diffuser had an inside diameter of 6.12 in. with its $(L/D)_d = 9$. One section of the 10.19-in. -diam diffuser contained a flanged port for installation of either of two total pressure rakes. Figure 5 shows the pressure rake installations used. In addition to these two diffuser configurations, one test was made with the expansion-deflection nozzle in a 30-in. plenum chamber, and two tests were made in a 6-in. diffuser with a second throat [$A_{st}/A_d = 0.654$, $\theta_{st} = 6^\circ$, $(L/D)_{st} = 0.431$] located downstream of the expansion-deflection nozzle.

The nozzles were mounted on a movable section of inlet supply pipe which permitted the nozzle to be translated approximately 9.0 in. along the horizontal centerline of the cylindrical diffuser. The design of the O-ring seals in the telescoping sections permitted the nozzle to be positioned during a test without leakage into the cell. The position of the nozzle was indicated by a counter which registered the rotations of the actuating mechanism (see Fig. 3).

The code designation for the various ejector configurations is included in Table 1. A typical ejector configuration designation would be S1-P1-10, which indicates an annular nozzle having shroud number one, nozzle centerbody number one, and tested in a 10-in. diffuser. The designation E-D-10 indicates an expansion-deflection nozzle in a 10-in. diffuser. Tests with the second throat diffuser are identified by the second throat area ratio, A_{st}/A_d .

3.1.3 Instrumentation

The parameters measured during this investigation were: cell pressure, p_c ; exhaust pressure, p_{ex} ; nozzle total pressure, p_t ; rake pressures, p_r ; total temperature, T_t ; and static pressures along the nozzle wall, p_n . Table 3 contains the range of the measured parameters and the type of measuring instrument used for each.

3.2 EXPERIMENTAL PROCEDURE

Prior to each test the nozzle, test cell, and instrumentation lines were pressure checked to minimize the possibility of leakage. A vacuum check was also made prior to each test to further reduce the possibility of instrumentation leakage.

Inlet air was supplied from the RTF compressors at pressure, p_t , as high as 46 psia and at temperatures approximately 100°F. The ejectors exhausted into the RTF exhaust machines, which provided pressures as low as 7 mm Hg abs. An electrically operated throttling valve was used in the exhaust ducting to control the exhaust pressure, p_{ex} , at the exit of the ejector. The inlet supply pressure was manually controlled by a gate-type valve.

Prior to testing, the nozzle position counter was indexed to zero with the nozzle shroud lip set at station zero. During the test the maximum exhaust pressure, p_{ex} , at which the ejector became started was obtained for each ejector configuration at a given nozzle position and total pressure, p_t , by decreasing the exhaust pressure until the cell pressure, p_c , reached a minimum value. The exhaust pressure was then increased until the ejector again became unstated (where p_c started to increase) to determine the maximum operating exhaust pressure. This procedure was repeated at various levels of total pressure, p_t .

During tests to determine the effect of diffuser length on ejector performance, the nozzle was positioned to obtain small variations in diffuser length. The movable nozzle system was also used to position the nozzle with respect to the second throat and the total pressure rakes.

4.0 DISCUSSION OF EXPERIMENTAL RESULTS

4.1 EJECTOR STARTING AND OPERATING CHARACTERISTICS

An ejector-diffuser system is defined as started when the expanded free jet boundary of the nozzle attaches to the diffuser wall such that the cell pressure becomes a minimum value for a given nozzle total pressure and is not affected by reductions of the exhaust pressure. Figure 6 illustrates this fundamental ejector starting phenomenon. As the ratio, p_{ex}/p_t , was decreased the nozzle became started (minimum nozzle exit pressure) at point "a", and the ejector became started (minimum cell pressure) at point "b" which corresponds to the ejector starting pressure ratio, $(p_{ex}/p_t)_{start}$. As the ratio, p_{ex}/p_t , was increased after the ejector started, the reverse of the described phenomenon occurred, and the ejector became unstated at point "c", which corresponds to the ejector operating pressure ratio, $(p_{ex}/p_t)_{oper}$. If the diffuser length to diameter ratio is maintained above approximately $(L/D)_d = 9$ (depending upon the nozzle geometry), an insignificant amount of hysteresis will exist, and thus point "b" will

coincide with "c" (see Ref. 3). Although the ejector starting characteristics for ejector systems using annular nozzles were similar to those of the more conventional nozzles, the flow field downstream of the E-D nozzle was affected during the starting phase because of the closing of the subsonic core behind the nozzle plug. Figure 2 shows a typical variation in plug base pressure and cell pressure when an ejector system using an E-D nozzle is started and unstated.

4.1.1 Effect of Diffuser Length

The effect of diffuser length on the ejector starting and operating characteristics of the annular nozzles tested is shown in Fig. 7. For nozzle configurations S2-P1, S3-P1, and S4-P1 the ejector starting and operating pressure ratio decreased as $(L/D)_d$ was decreased; however, no significant hysteresis existed. For both the E-D nozzle and the S1-P1 nozzle, the starting pressure ratios decreased greatly as $(L/D)_d$ was decreased, resulting in a significant amount of hysteresis. Unfortunately, these data contain three variables, including the amount of external self adjustment, nozzle exit angle, and nozzle exit diameter. Any one of these variables could influence the amount of hysteresis. Figure 8a further shows the effect of this hysteresis on the ejector starting characteristics for an annular nozzle configuration as the diffuser length was decreased from $(L/D)_d = 9$ to $(L/D)_d = 6$. A region of ejector instability accompanied this large hysteresis just prior to starting the ejector. However, it should be noted that this instability is not necessarily related to the hysteresis. Figure 8b shows that instability also occurs for nozzle configurations which have no hysteresis at diffuser lengths below $(L/D)_d = 6$. Similar ejector instability was reported in Ref. 1 for C-D nozzles operating with $(L/D)_d = 3$. Because an annular nozzle ejector system may be operated in this unstated region to simulate a lower altitude than that obtained when the ejector is started, the length of a cylindrical diffuser should be approximately $(L/D)_d = 9$ to avoid this region of instability.

4.1.2 Calculation of Ejector Starting Pressure Ratio

For a compression shock system in a long duct, Shapiro (Ref. 7) states that one-dimensional normal shock relationship used with the duct inlet Mach number will predict the pressure rise across the shock system within six percent. Although Shapiro's results were obtained for uniform duct inlet flow, the experimental results for ejectors in which the inlet flow was not uniform still showed good agreement with one-dimensional normal shock relationships.

For ejectors having no subsonic diffuser, it was assumed that the ejector system diffused to the exhaust conditions in a manner proportional to the static-to-total pressure ratio across a normal shock for

the isentropic inlet Mach number corresponding to A_d/A^* . Reference 3 shows that a correction to the one-dimensional normal shock pressure ratio for nozzle exit angle was required to determine the ejector starting pressure ratio for C-D nozzles. Thus, a similar correction factor for annular nozzle-ejector systems operating without a subsonic diffuser can be defined as

$$K = (p_{ex}/p_t)_{\text{exper}} / (p_2/p_{t_1})_{ns} \quad (1)$$

where

$$(p_2/p_{t_1})_{ns} = f(A_d/A^*)$$

When this procedure is used, Fig. 9 shows that both the nozzle exit angle and the external nozzle spike appear to have a strong influence on the correction factor.

Although no theory or new empirical relationship is presented to predict the ejector starting pressure ratio accurately for annular nozzles, the assumption of a correction to the normal shock pressure ratio of $K = 0.90$ for $(L/D)_d \geq 9$ would give a maximum error of ± 8 percent in the starting pressure ratio for the configurations tested. Figure 10 further shows a comparison with C-D nozzle data for the correction constant required to calculate the ejector starting and operating pressure ratio for the various annular nozzle ejector configurations tested as a function of $(L/D)_d$.

4.2 EJECTOR PUMPING CHARACTERISTICS

4.2.1 Reynolds Number Effect on Cell Pressure

The definition of a started ejector system states that for a given nozzle total pressure the cell pressure ratio is a minimum and is not influenced by changes in exhaust pressure. However, the ratio of cell pressure to nozzle total pressure can vary with nozzle total pressure because of the Reynolds number effect reported in Ref. 4. Figure 11 shows the variation of minimum cell pressure ratio with Reynolds number for the various annular nozzles tested.

4.2.2 Diffuser Length Effect on Cell Pressure

Figure 11 also shows that the cell pressure was influenced by diffuser length. A similar effect on cell pressure was noted for C-D nozzles in Ref. 3.

The variation of cell pressure with diffuser length is not fully understood, and no explanation can be offered at the present time to substantiate the data.

4.2.3 Minimum Cell Pressure Calculation

The minimum cell pressure ratio was calculated for each ejector configuration tested using the empirical correction factor developed for 18-deg conical nozzles in Ref. 4. This correction assumes that the gas expands isentropically to a fictitious duct area which may be calculated by multiplying the actual duct area by K' Eq. (2).

$$K' = \frac{1 - \frac{3}{2} e^{-3.89 R_{ne} (D^*/D_{ne}) 10^{-6}} + \frac{1}{2} e^{-R_{ne} (D^*/D_{ne}) 10^{-6}}}{(D_d/D_{ne})^{0.25}} + \frac{\frac{1}{2} e^{-R_{ne} (D^*/D_{ne}) 10^{-5}}}{(D_d/D_{ne})^{0.25}} \quad (2)$$

Equation (3) is the isentropic relation between the pressure ratio and the fictitious area ratio.

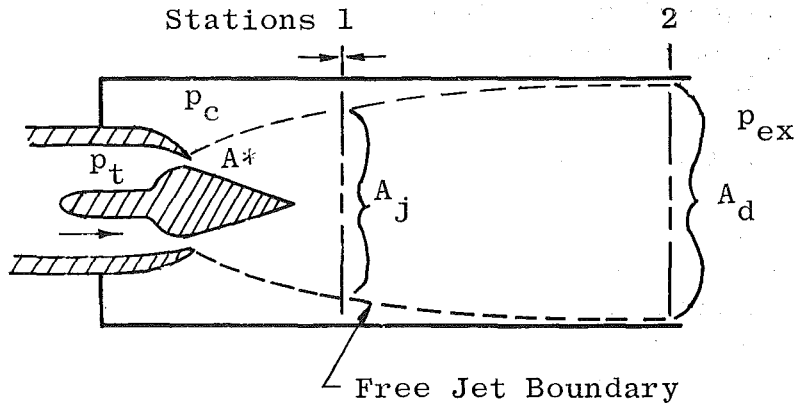
$$K' \left(\frac{A_d}{A^*} \right) = \sqrt{\left(\frac{\gamma-1}{2} \right) \left(\frac{2}{\gamma+1} \right)^{\frac{\gamma+1}{\gamma-1}}} \left(\frac{p_c}{p_t} \right)^{\frac{1}{\gamma}} \sqrt{1 - \left(\frac{p_c}{p_t} \right)^{\frac{\gamma-1}{\gamma}}} \quad (3)$$

Because of the difficulty in determining the pressure ratio from Equation (3), it is suggested that the fictitious area ratio and compressible flow tables be used.

The comparison of the calculated cell pressure ratio with the experimental values (Fig. 12) shows that an additional correction for the nozzle exit angle, similar to that required for C-D nozzles, is necessary.

4.2.4 Cell Pressure Calculation for Unstarted Ejector

The annual nozzle test requirement for altitude simulation at conditions other than minimum cell pressure makes it very desirable to determine the relationship between diffuser exhaust pressure and cell pressure when the ejector is unstarted. For diffuser lengths of approximately nine diffuser diameters $[(L/D)_d \approx 9]$, the exhaust pressure ratio for a given cell pressure ratio may be estimated by applying the conservation of mass, momentum, and energy between stations one and two.



To simplify the solution of the conservation equations the following assumptions are made:

1. Flow is steady.
2. Gas is perfect.
3. Flow is adiabatic.
4. Flow is one dimensional within the expanding free jet at stations one and two.
5. Static pressure at station one is constant and equal to cell pressure. (Note: The desired cell pressure must be greater than the minimum cell pressure.)
6. Flow is isentropic from nozzle to station one.
7. Diffuser wall friction is negligible.
8. Flow at station two fills the diffuser.
9. Static pressure at station two equals exhaust pressure.
10. Velocity in cell region at station one is zero.

Based on the above assumptions the total force at stations one and two may be written and equated.

$$F_1 = p_c A_j (1 + \gamma M_j^2) + p_c (A_d - A_j) \quad (4)$$

or

$$F_1 = p_c (A_d + A_j \gamma M_j^2) \quad (5)$$

and also

$$F_2 = p_{ex} A_d (1 + \gamma M_2^2) \quad (6)$$

Equating Eqs. (5) and (6),

$$p_c (A_d + A_j \gamma M_j^2) = p_{ex} A_d (1 + \gamma M_2^2) \quad (7)$$

From continuity the mass flow at stations one and two may be written:

$$m_1 = \sqrt{\gamma/RT_j} \quad p_c A_j M_j \quad (8)$$

and

$$m_2 = \sqrt{\gamma/RT_2} \quad p_{ex} A_d M_2 \quad (9)$$

Equating Eqs. (8) and (9),

$$\sqrt{\gamma/RT_j} \quad p_c A_j M_j = \sqrt{\gamma/RT_2} \quad p_{ex} A_d M_2 \quad (10)$$

From the conservation of energy and the preceding assumptions, it may be stated that

$$T_j = \frac{T_t}{1 + \frac{\gamma-1}{2} M_j^2} \quad (11)$$

and

$$T_2 = \frac{T_t}{1 + \frac{\gamma-1}{2} M_2^2} \quad (12)$$

Combining Eqs. (7), (10), (11), and (12)

$$\frac{A_d/A_j + \gamma M_j^2}{M_j \sqrt{1 + \frac{(\gamma-1)}{2} M_j^2}} = \frac{1 + \gamma M_2^2}{M_2 \sqrt{1 + \frac{(\gamma-1)}{2} M_2^2}} \quad (13)$$

where

$$M_j^2 = \frac{2}{\gamma-1} \left[\left(\frac{p_t}{p_c} \right)^{\frac{\gamma-1}{\gamma}} - 1 \right] \quad (14)$$

and

$$A_j = A^* \left(\frac{p_c}{p_t} \right)^{-\frac{1}{\gamma}} \sqrt{\frac{\left(\frac{\gamma-1}{2} \right) \left(\frac{2}{\gamma+1} \right)^{\frac{\gamma+1}{\gamma-1}}}{1 - \left(\frac{p_c}{p_t} \right)^{\frac{\gamma-1}{\gamma}}}} \quad (15)$$

When Eqs. (13), (14), and (15) are used, the Mach number at station two may be determined as a function of cell pressure with all other quantities being known. For this case the subsonic solution for M_2 using Eq. (13) is the solution of interest since, from Eq. (7), it allows the maximum diffuser exhaust pressure. Figure 13 presents a

graphical solution for the positive subsonic Mach number at station two from Eq. (13) for various values of γ . With the Mach number at station two thus obtained, the exhaust pressure required for the assumed cell pressure may be calculated from either Eq. (7) or (9). Obviously, the assumed cell pressure must be greater than the minimum cell pressure obtainable by the ejector system (see section 4.2.3).

In Figs. 14a and b, the experimental ejector pumping characteristics for several annular nozzle configurations are compared with the theoretical starting curve obtained from this simplified flow model. It should be noted that the rate of change of cell pressure with respect to exhaust pressure is quite high when the ejector system nears the starting conditions. This results in a large deviation in cell pressure for a small error or variation in exhaust pressure. For this reason the above methods should be considered to be only a first approximation. The regulation of cell pressure with exhaust pressure for an unstarted ejector system is not necessarily the best technique for controlling cell pressure due to this high rate of change in cell pressure with exhaust pressure during certain regions.

4.3 EFFECT OF EJECTOR-DIFFUSER ON E-D NOZZLE PERFORMANCE

4.3.1 Effect of Diffuser Diameter

The expansion-deflection nozzle (Ref. 6) was tested in a large plenum chamber (Config. E-D-30) with an inside diameter 7.15 times that of the nozzle exit diameter. This test was conducted to determine the relation between cell pressure and nozzle wall static pressures when the latter were unaffected by the presence of an ejector diffuser. The E-D nozzle was then tested in two diffusers having inside diameters 1.46 and 2.84 times that of the nozzle exit diameter. (Configs. E-D-6 and E-D-10). These diffusers were sufficiently small to allow the ejector to operate in the started mode (Regime 3 - ejector started; plug wake closed). The influence of these diffuser configurations on nozzle wall pressure is shown in Fig. 15. The pressures at four axial stations are shown where each point represents an average of two pressures at the same axial station 180-deg apart in the nozzle. In this regime as well as in Regime 2 (ejector unstarted, plug wake closed), it may be seen from these data that the nozzle wall static pressures are independent of cell pressure. Under these conditions the size of the diffuser has no effect on nozzle performance. As the cell pressure was increased, the wake behind the nozzle plug opened (Regime 1), and the nozzle wall pressures also increased. Figure 15 shows the pressure at the two nozzle wall stations nearest the nozzle

exit to be slightly higher for configurations E-D-6 and E-D-10. As the cell pressure was increased further, the nozzle wall static pressure nearest the nozzle exit of configuration E-D-6 was higher than that of configuration E-D-10. This indicates that as the diffuser diameter approaches the nozzle exit diameter, an increased effect on nozzle performance exists when the system is operating in Regime 1. This effect on nozzle wall pressures is attributed to the influence of the diffuser on the closing mechanism of the central subsonic core, which is located downstream of the nozzle, and allows the higher downstream pressures to be fed through the subsonic core and influence nozzle performance.

4.3.2 Effect of Second Throat on E-D Nozzle

Ejector configuration E-D-6 was tested with a second throat ($A_{st}/A_d = 0.654$) located at two positions. Figure 16 shows that when a second throat was located close to the E-D nozzle (at 1.11 nozzle diameters) the relationship between cell pressure and nozzle wall static pressure in regime 1 was drastically altered. This influence on the nozzle pressures would make any measurement of performance invalid. When the second throat was moved downstream (at 3.57 nozzle diameters), the second throat had no effect upon the nozzle wall static pressures. The Mach number along the centerline of the E-D nozzle jet was calculated from measured total and static pressures when the nozzle was operated in a 10-inch diffuser at a total pressure of 40 psia and is presented in Fig. 17. This figure shows that the subsonic core extends approximately 1.5 nozzle diameters downstream of the nozzle exit when the ejector is operated in regime 1 (ejector unstarted, plug wake open). When the second throat is positioned upstream of the closing point of this subsonic core (1.11 nozzle diameters), the disturbance to the flow is fed upstream and affects nozzle performance.

5.0 CONCLUSIONS

As a result of the investigation to determine the performance of ejector-diffuser systems using an annular driving nozzle, the following conclusions may be reached:

1. The ejector starting pressure ratio for $(L/D)_d \geq 9$ can be estimated within ± 8 percent for the configurations tested by applying an empirical correction of $K = 0.90$ to the normal shock pressure ratio. The diffuser inlet conditions are assumed to be an isentropic function of the ratio of diffuser area to nozzle throat area.

2. The pressure ratio required for starting the ejector decreases as the diffuser length to diameter ratio decreases below approximately $(L/D)_d = 9$. Below this diffuser length, a region of instability sometimes occurs when the ejector is unstarted.
3. The minimum cell pressure can be approximated by using an empirical equation, which has been used by investigators to determine the ejector pumping characteristics for convergent-divergent nozzles, and by applying a correction for nozzle exit angle.
4. The relationship between the cell pressure and exhaust pressure for an unstarted ejector can be estimated using one-dimensional conservation equations.
5. When the central subsonic core behind the plug extends downstream of the exit of the E-D nozzle, the diffuser diameter should be made as large as possible in comparison to the nozzle exit diameter to minimize any influence of the diffuser on nozzle performance.
6. It was necessary to locate the inlet to the second throat downstream of the closing point of the E-D nozzle subsonic core when the ejector is unstarted to eliminate the influence of the second throat on nozzle performance. The closing point of the subsonic core was found to be approximately 1.5 nozzle diameters downstream of the nozzle exit when the nozzle was operated in a 10-in. diffuser at a total pressure of 40 psia.

REFERENCES

1. Barton, D. L. and Taylor, D. "An Investigation of Ejectors without Induced Flow, Phase I." AEDC-TN-59-145, December 1959.
2. Taylor, D., Barton, D. L., and Simmons, M. "An Investigation of Cylindrical Ejectors Equipped with Truncated Conical Inlets, Phase II." AEDC-TN-60-224, March 1961.
3. German, R. C. and Bauer, R. C. "Effects of Diffuser Length on the Performance of Ejectors without Induced Flow." AEDC-TN-61-89, August 1961.

4. Bauer, R. C. and German, R. C. "Some Reynolds Number Effects on the Performance of Ejectors without Induced Flow." AEDC-TN-61-87, August 1961.
5. Bauer, R. C. and German, R. C. "The Effect of Second Throat Geometry on the Performance of Ejectors without Induced Flow." AEDC-TN-61-133, November 1961.
6. Rao, G. V. R. "Recent Developments in Rocket Nozzle Configurations." ARS Journal, Vol. 31, No. 11, pp. 1488-1494, November 1961.
7. Shapiro, A. H. The Dynamics and Thermodynamics of Compressible Fluid Flow, Vol. I. The Ronald Press Company, New York, 1953.

TABLE 1

DESCRIPTION OF EJECTOR-DIFFUSER TEST CONFIGURATIONS

Ejector Designation	Diffuser Diam., D_d	A_d/A^*	$(L/D)_d$	Nozzle Configuration		θ_{ne} deg	$(D_{ne})_{eff}^{\dagger}$ in.	$(D^*)_{eff}$ in.	A_{ne}/A^*
				Shroud	Centerbody				
S1-P1-10	10.19	153.5	3.0, 6.0, 9.0	1	1	11.3	4.160	.822	25.6
S2-P1-10		"		2	1	18.5	3.546	"	18.6
S3-P1-10		"		3	1	34.6	2.135	"	6.8
S4-P1-10		144.1	3.0, 6.0, 9.0	4	1	-27.0	.896	.849	1.1
S1-P2-10		153.5	9.0	1	2	11.3	4.160	.822	25.6
S2-P2-10		"	"	2	2	18.5	3.614	"	19.3
S1-P3-10		"	"	1	3	11.3	4.160	"	25.6
E-D-10	10.19	118.2	3.0, 6.0, 9.0	-	-	8	4.196	.937	20.0
E-D-30	29.25 Diam x 53.0 Long Plenum Chamber (Ejector did not start.)								
S1-P1-6	6.12	55.4	9.0	1	1	11.3	4.160	.822	25.6
S2-P1-6		"		2	1	18.5	3.546	"	18.6
S3-P1-6		"		3	1	34.6	2.135	"	6.8
S4-P1-6		52.0		4	1	-27.0	.896	.849	1.1
E-D-6 ⁺	6.12	42.6	9.0	-	-	8	4.196	.937	20.0

$$^{\dagger} (D_{ne})_{eff} = (D_s^2 - D_{pe}^2)^{1/2}$$

+ Configuration used during second throat tests ($A_{st}/A_{\ell} = 0.654$, $\theta_{st} = 6^\circ$, $(L/D)_{st} = 0.431$)

TABLE 2
DESCRIPTION OF ANNULAR NOZZLES

Nozzle Config.		A_{ne}/A^*_{eff}	θ_{ne} deg	θ_p deg	$D^*_{eff} \dagger$	D_s	D_{pe}	D_{p^*}	X_p	ℓ/X_p	θ^*
Shroud	Centerbody										
1	1	25.6	11.3	17.5	0.822	4.160	0	1.698	2.681	0	30
2	1	18.6	18.5	"	"	3.614	0.698	"	"	0.403	30
3	1	6.8	34.6	"	"	2.597	1.48	"	"	0.854	30
4	1	1.1	-27	"	0.849	1.849	1.619	1.619	2.491	1.0	-27
1	2	25.6	11.3	30.0	0.822	4.160	0	1.698	1.600	-0.675	30
2	2	19.3	18.5	"	"	3.614	0	"	"	0	30
1	3	25.6	11.3	-	"	4.610	0	"	0.39	-5.88	30
E-D (Expansion-Deflection)		20.0	8	-	0.937	4.196	0	1.643	-	-11.35	75

\dagger The effective throat diameter was determined by measuring the mass flow through the nozzle with a calibrated venturi.

See Fig. 4 for dimensional details.

TABLE 3
DESCRIPTION OF MEASURING INSTRUMENTS

Parameter Measured	Range Measured	Measuring Instrument
P_c	0.2 to 5mm Hg abs	McLeod (with nitrogen cold trap)
	5 to 50mm Hg abs	diaphragm-activated dial gage
P_{ex}	7 to 50mm Hg abs	diaphragm-activated dial gage
	1 to 10 psia	diaphragm-activated dial gage
P_t	1 to 46 psia	diaphragm-activated dial gage
P_n or P_r	0.1 to 90 in. Hg abs	manometer (mercury)
	0.1 to 90 in. Oil	manometer (silicone oil- sp. gr. = 1.092 at 80°F)
T_t	70 to 100°F	copper-constantan thermocouple

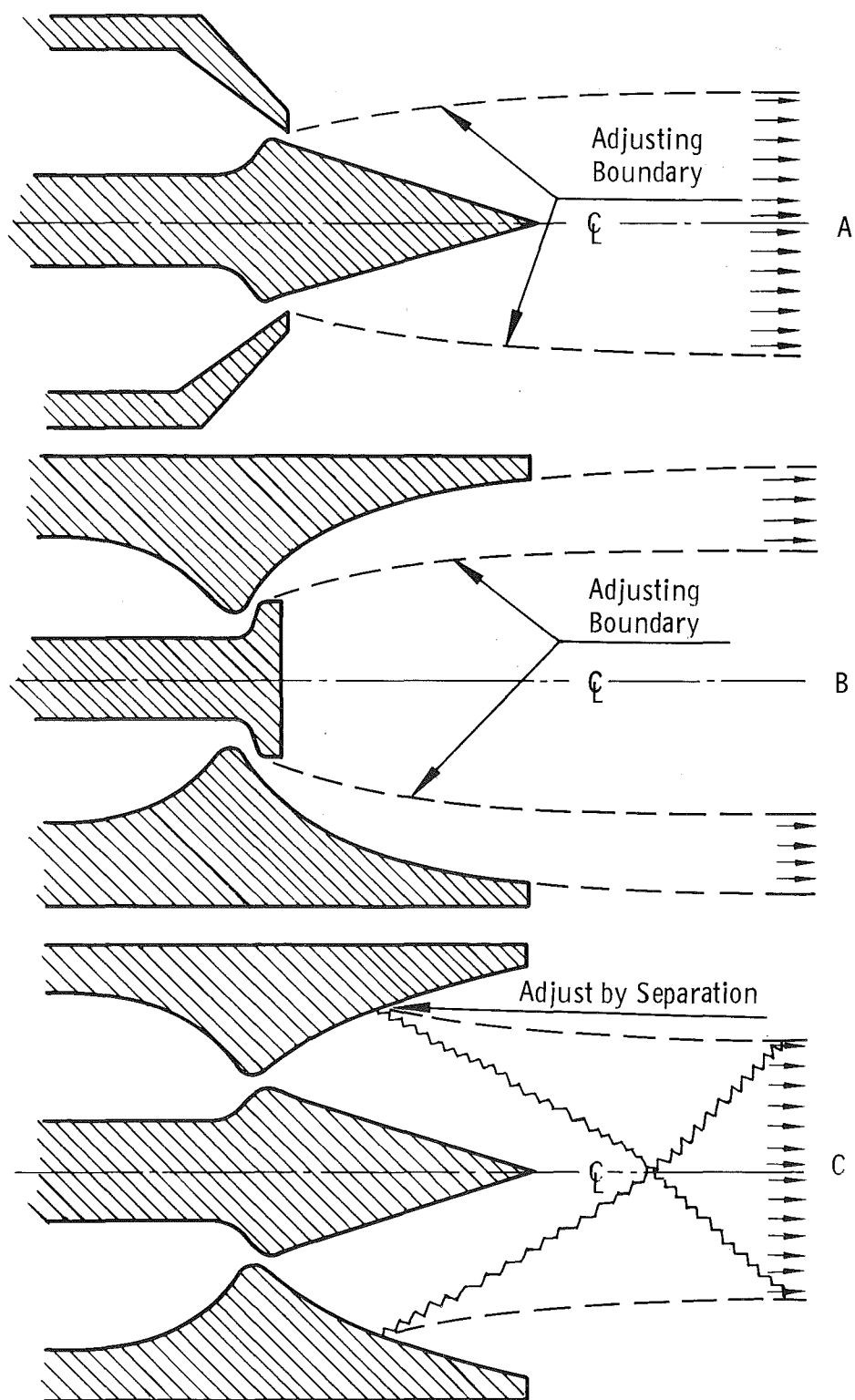


Fig. 1 Types of Annular Nozzles

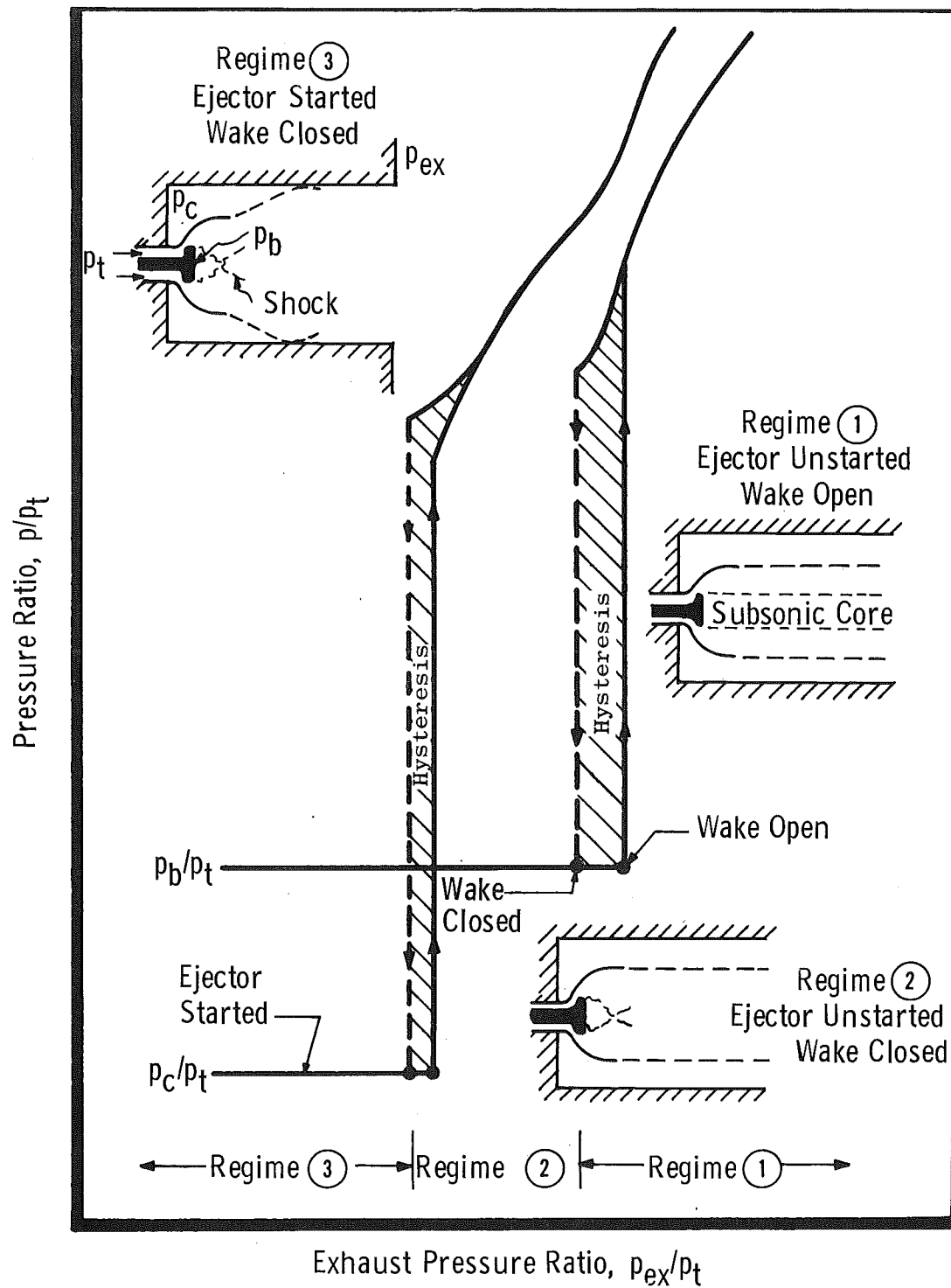


Fig. 2 Typical Operation of an Expansion-Deflection Nozzle in an Ejector-Diffuser System

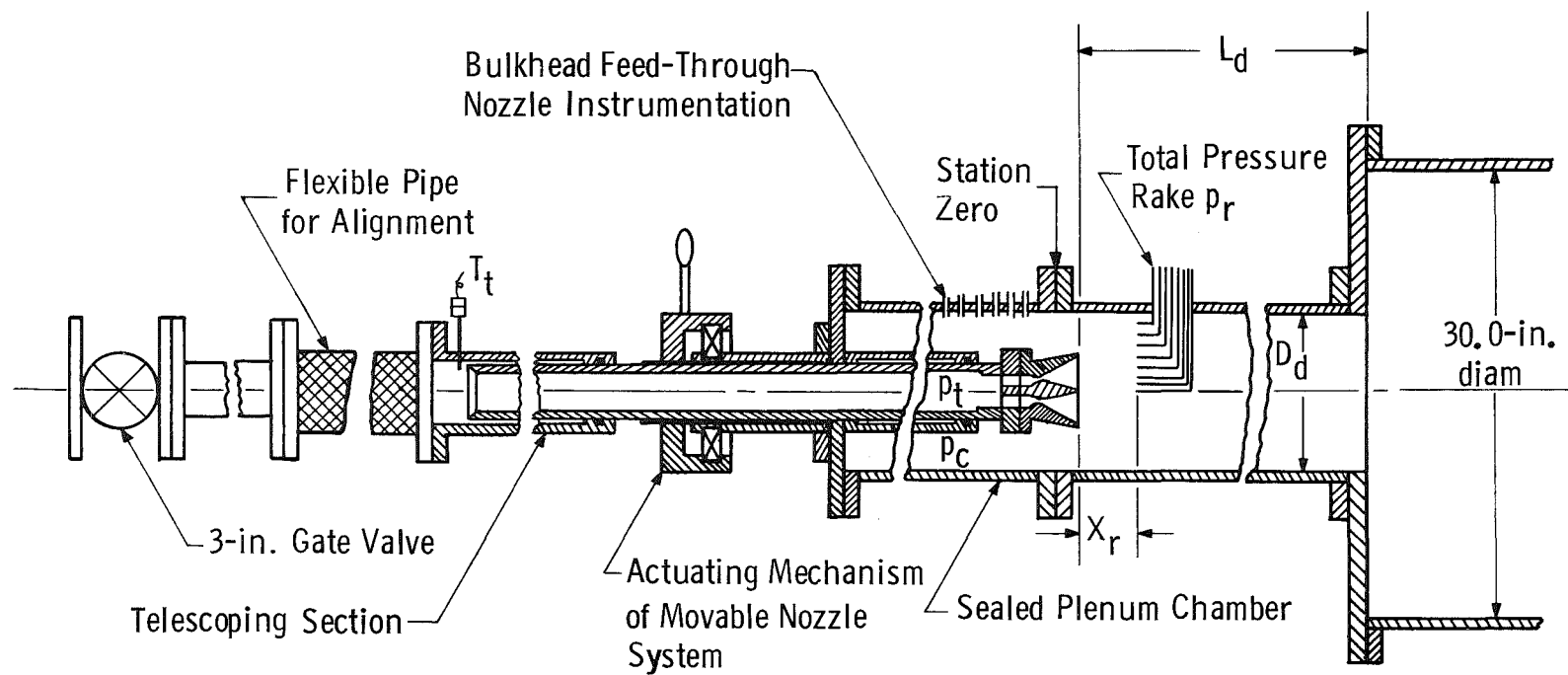


Fig. 3 Typical Ejector-Diffuser Test Configuration

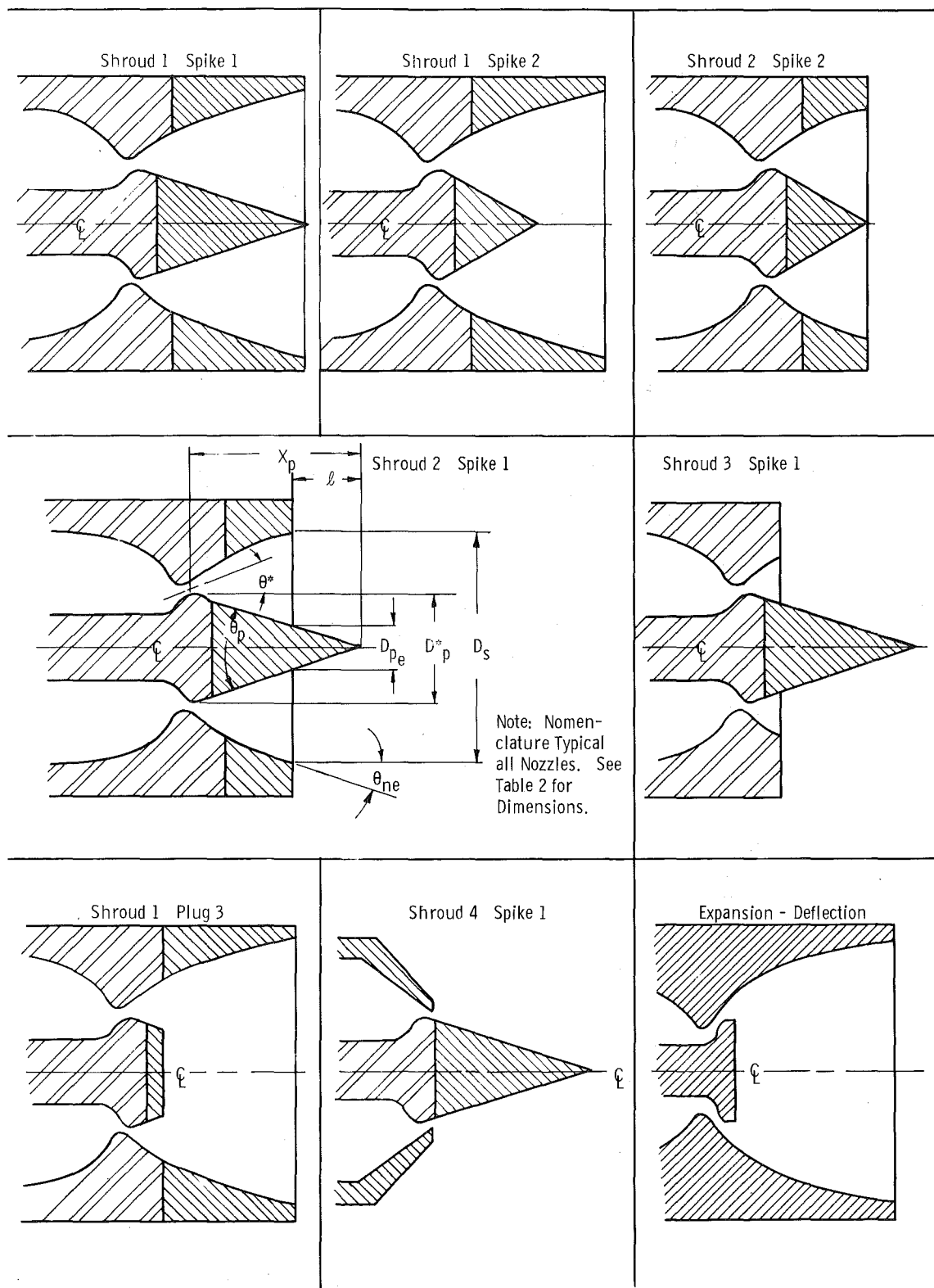


Fig. 4 Annual Nozzle Configurations Tested

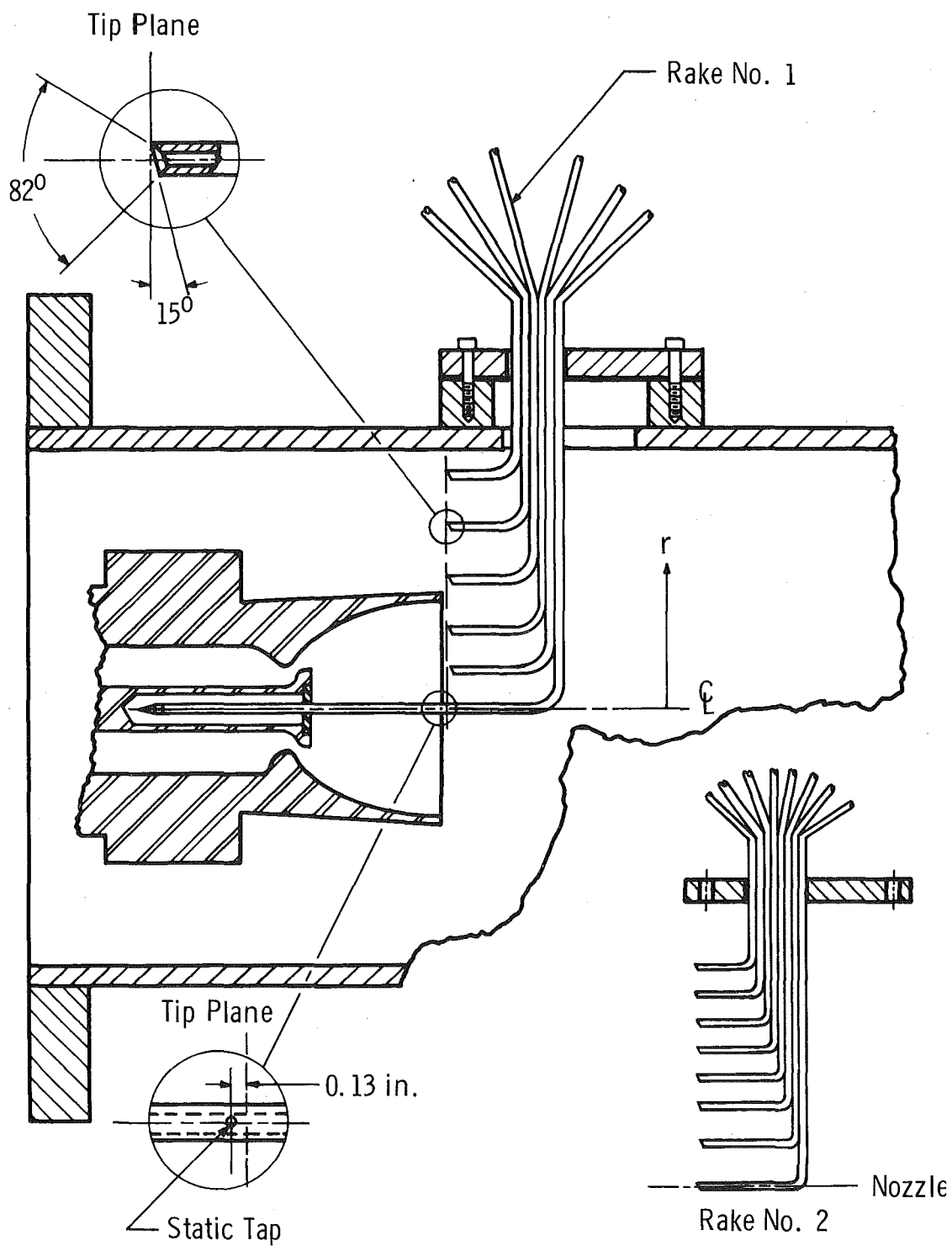


Fig. 5 Typical Total Pressure Rake Installation

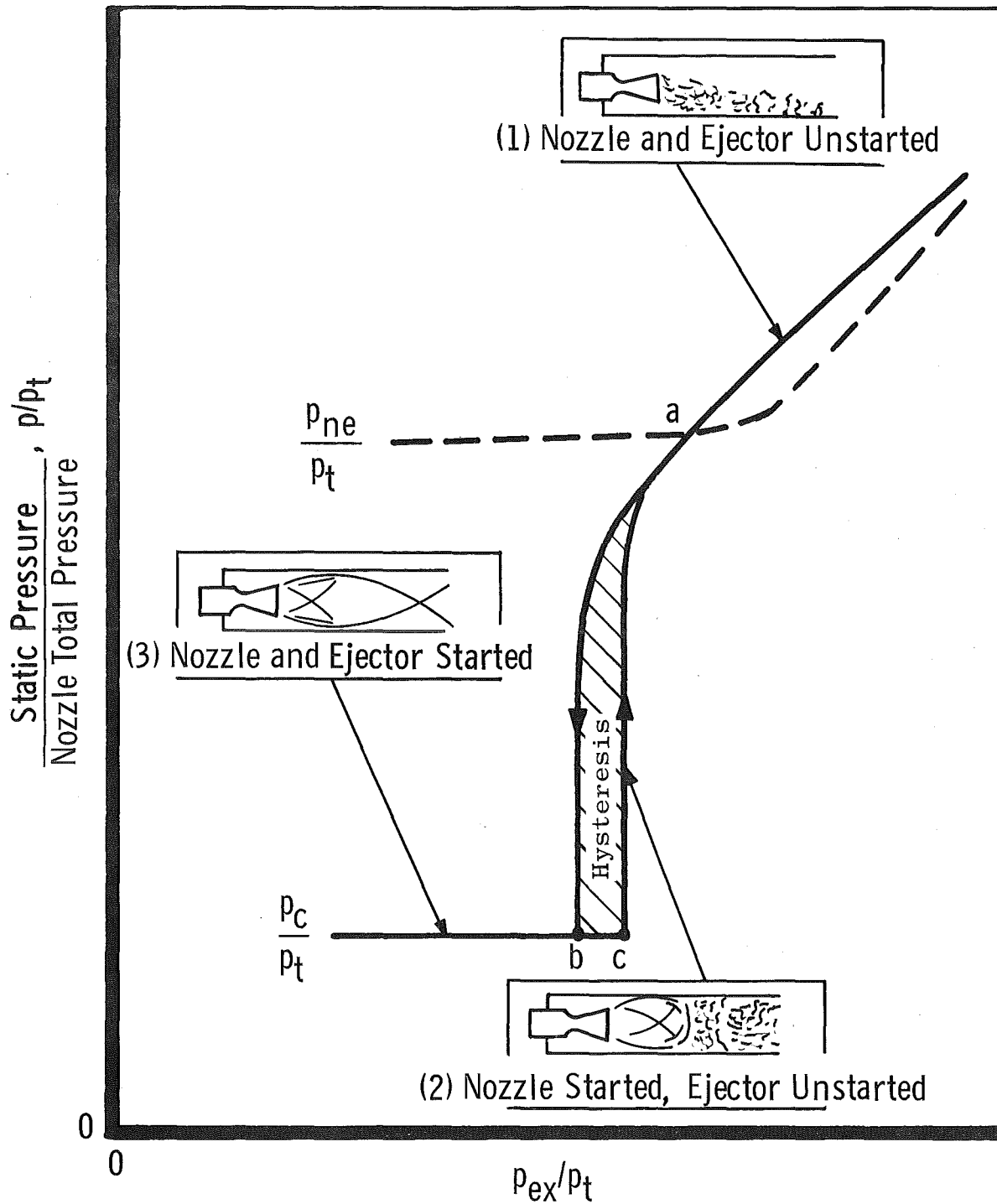


Fig. 6 Typical Ejector Starting Phenomenon for Constant Nozzle Total Pressure

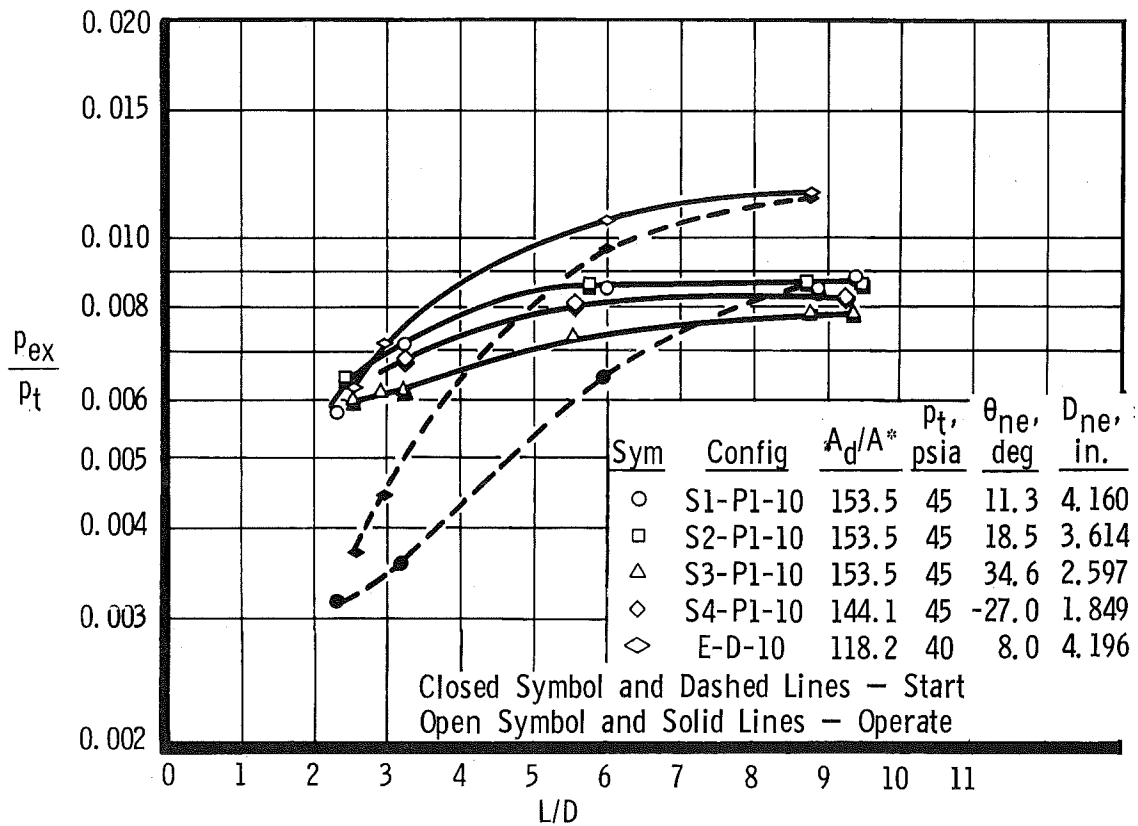
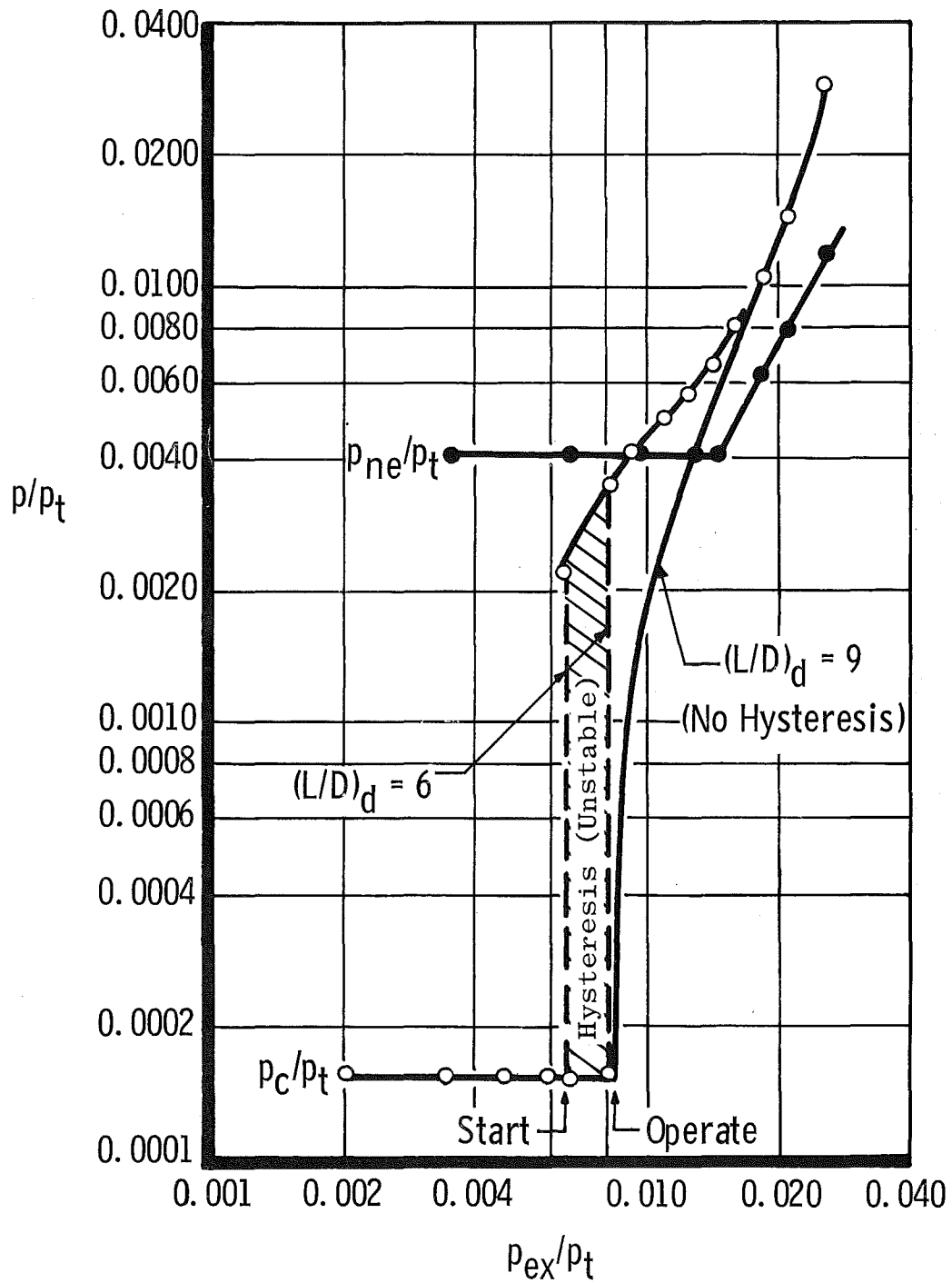
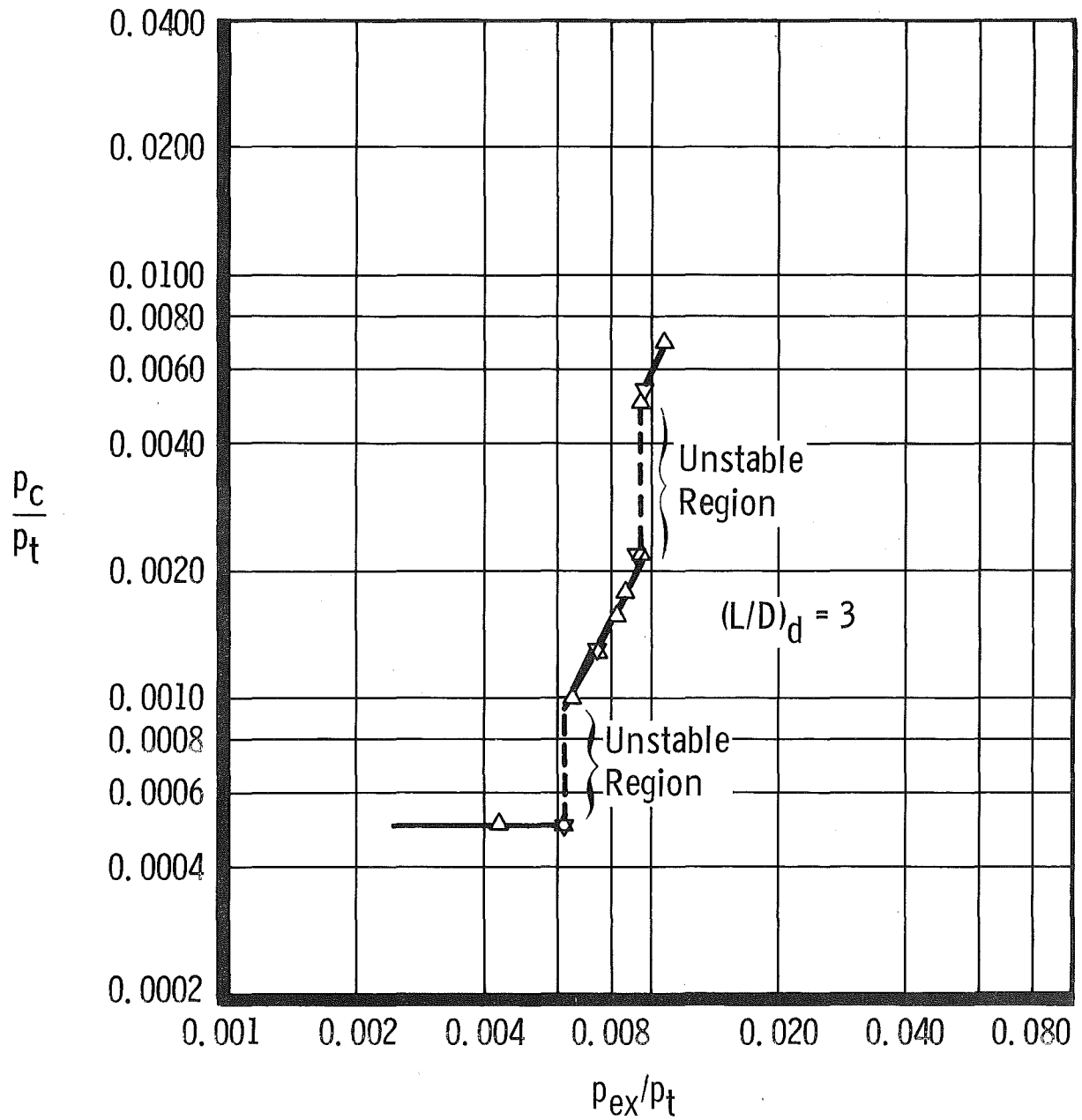


Fig. 7 Effect of Diffuser Length on Ejector Starting and Operating Pressure Ratio for Various Annular Nozzles



a. S1-P1-10 Ejector Configuration

Fig. 8 Effect of Diffuser Length on Ejector Starting Characteristics



b. S3-P1-10 Ejector Configuration

Fig. 8 Concluded

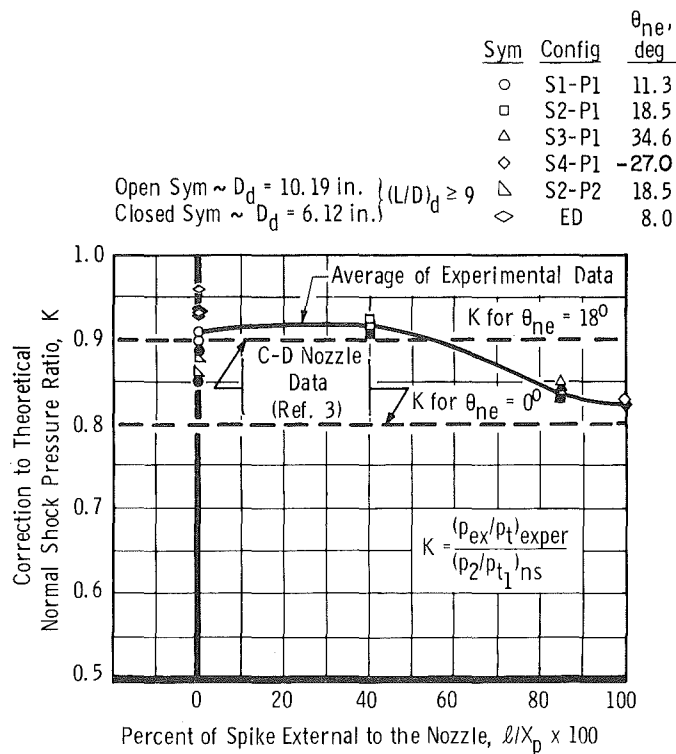


Fig. 9 Comparison of the Starting Pressure Ratio Correction Factor for Various Annual Nozzle Configurations with That Obtained for C-D Nozzles

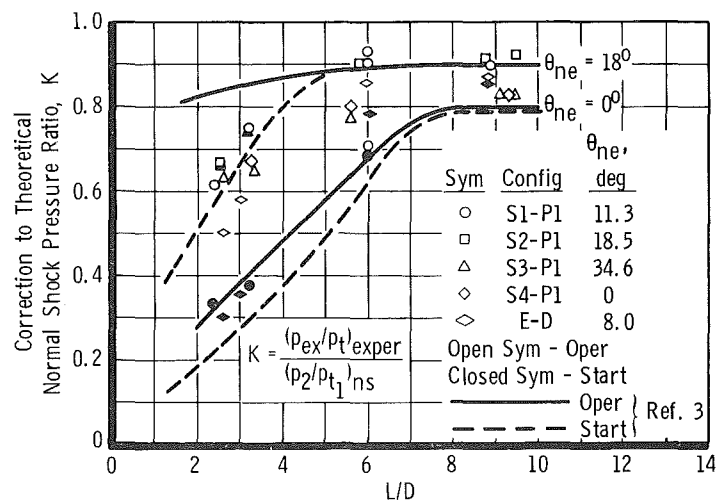


Fig. 10 Correction to Normal Shock Pressure Ratio Required for Various Diffuser Length Ratios

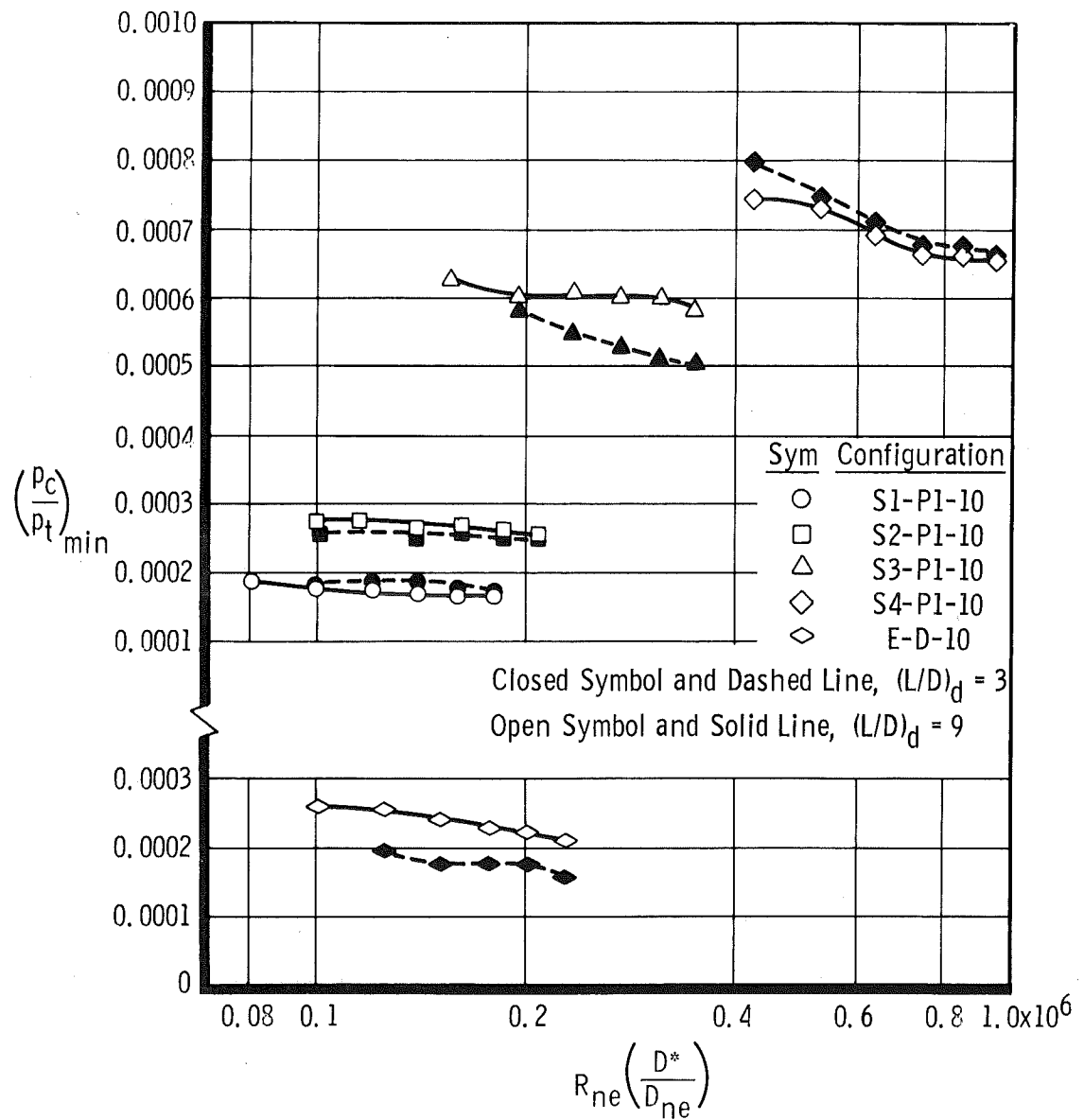


Fig. 11 Effect of Reynolds Number on Minimum Cell Pressure Ratio

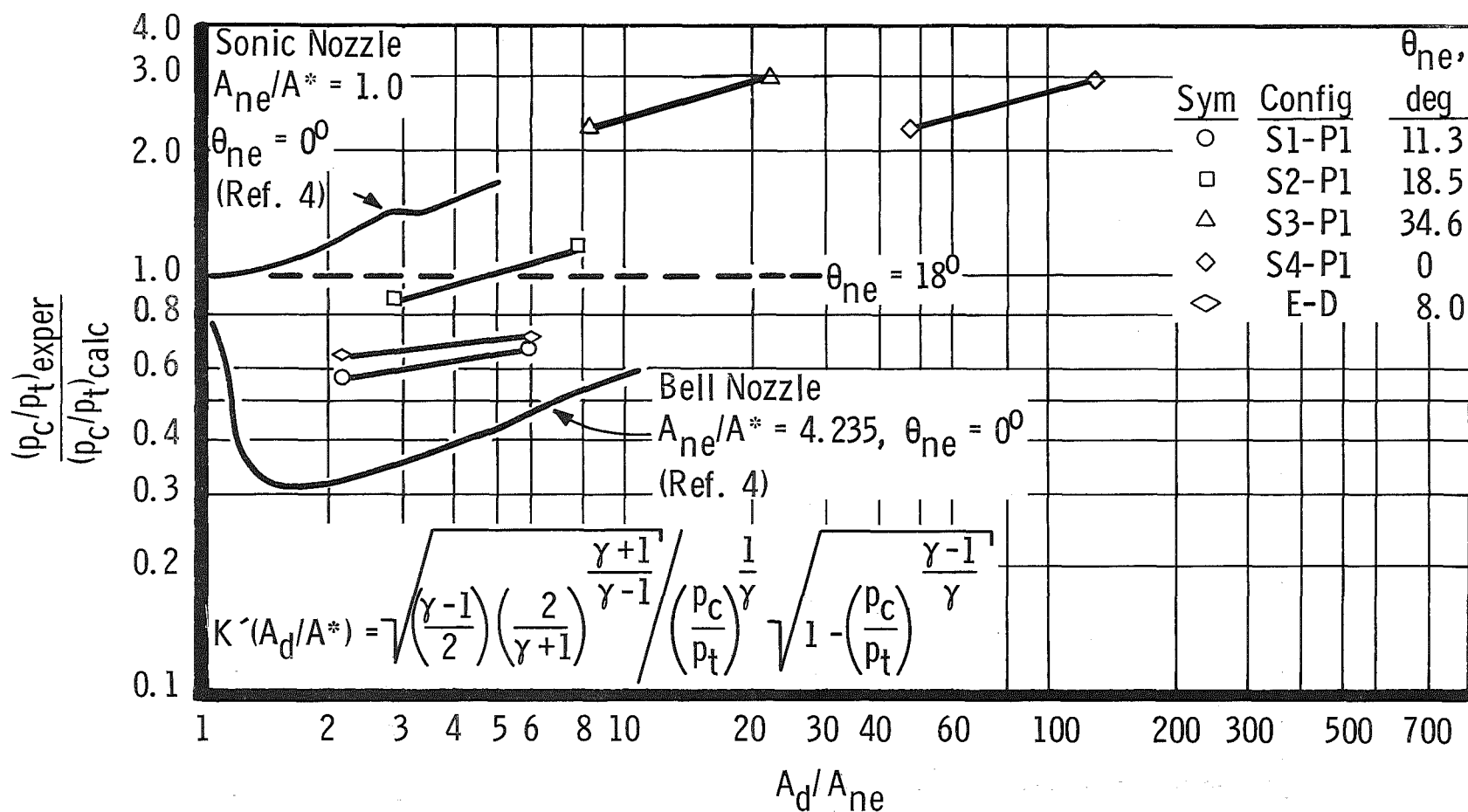


Fig. 12 Comparison of the Ratio of Experimental and Calculated Minimum Cell Pressure Ratio for Various Annular Nozzle Configurations with That Obtained for C-D Nozzles

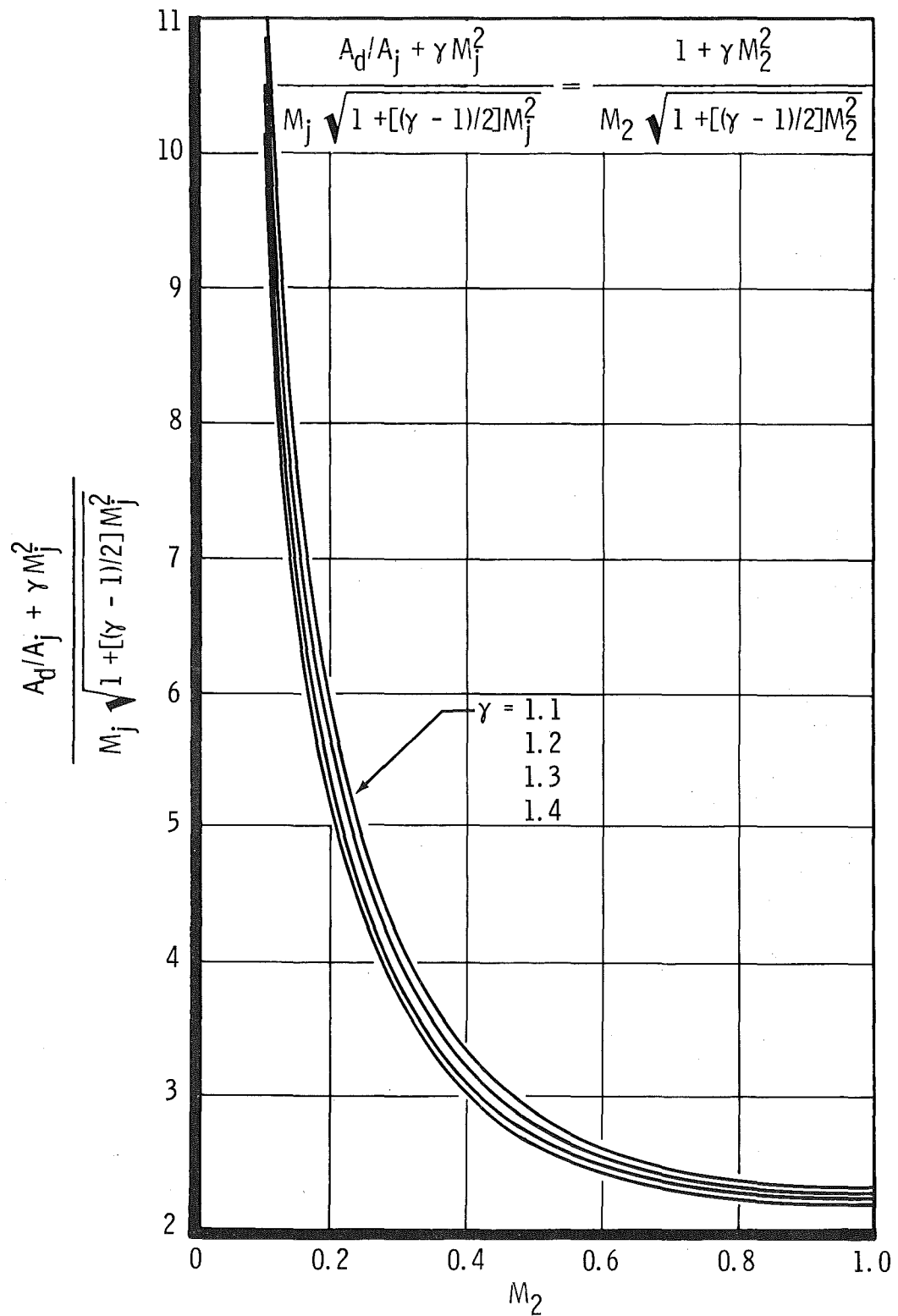
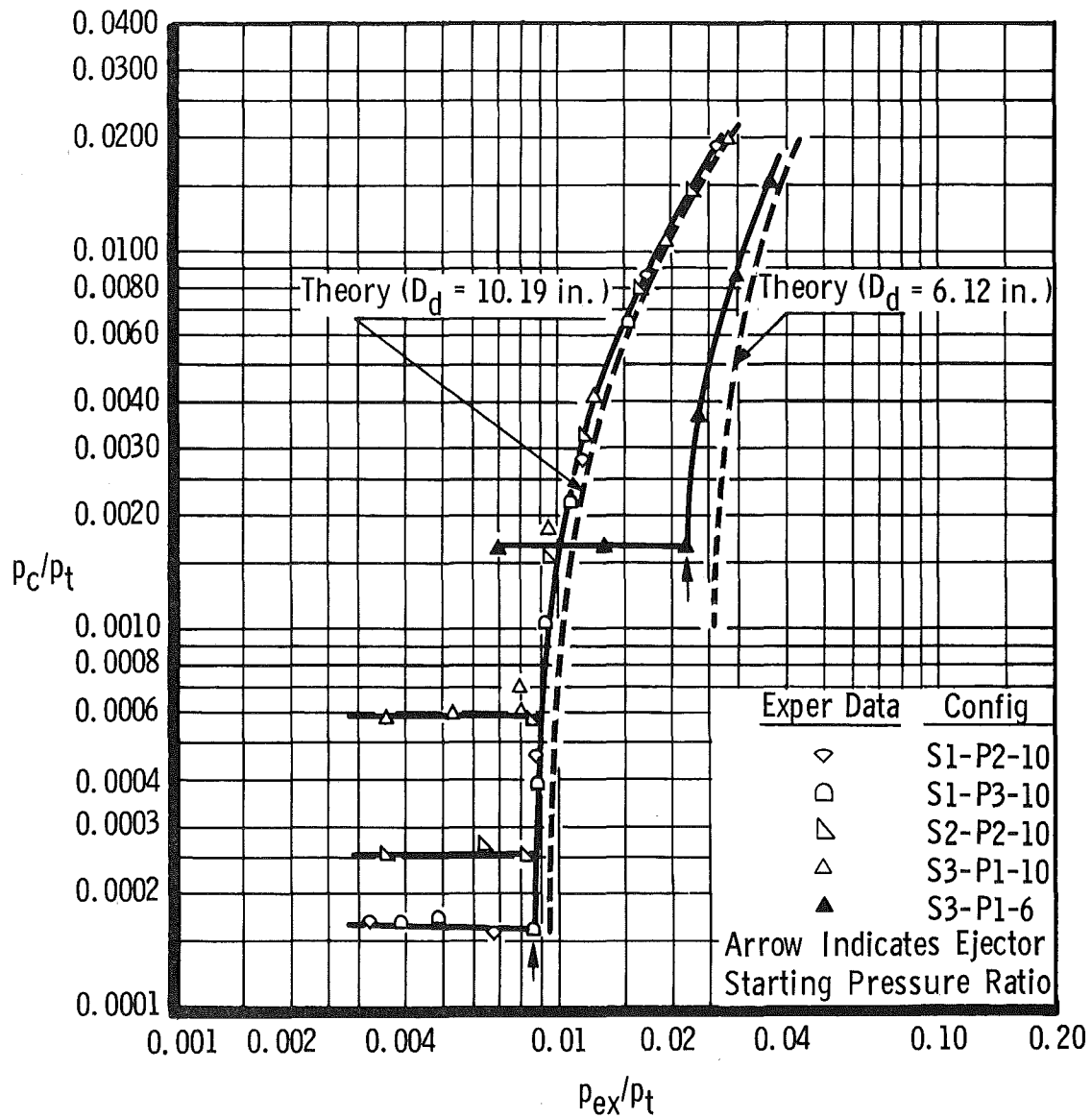
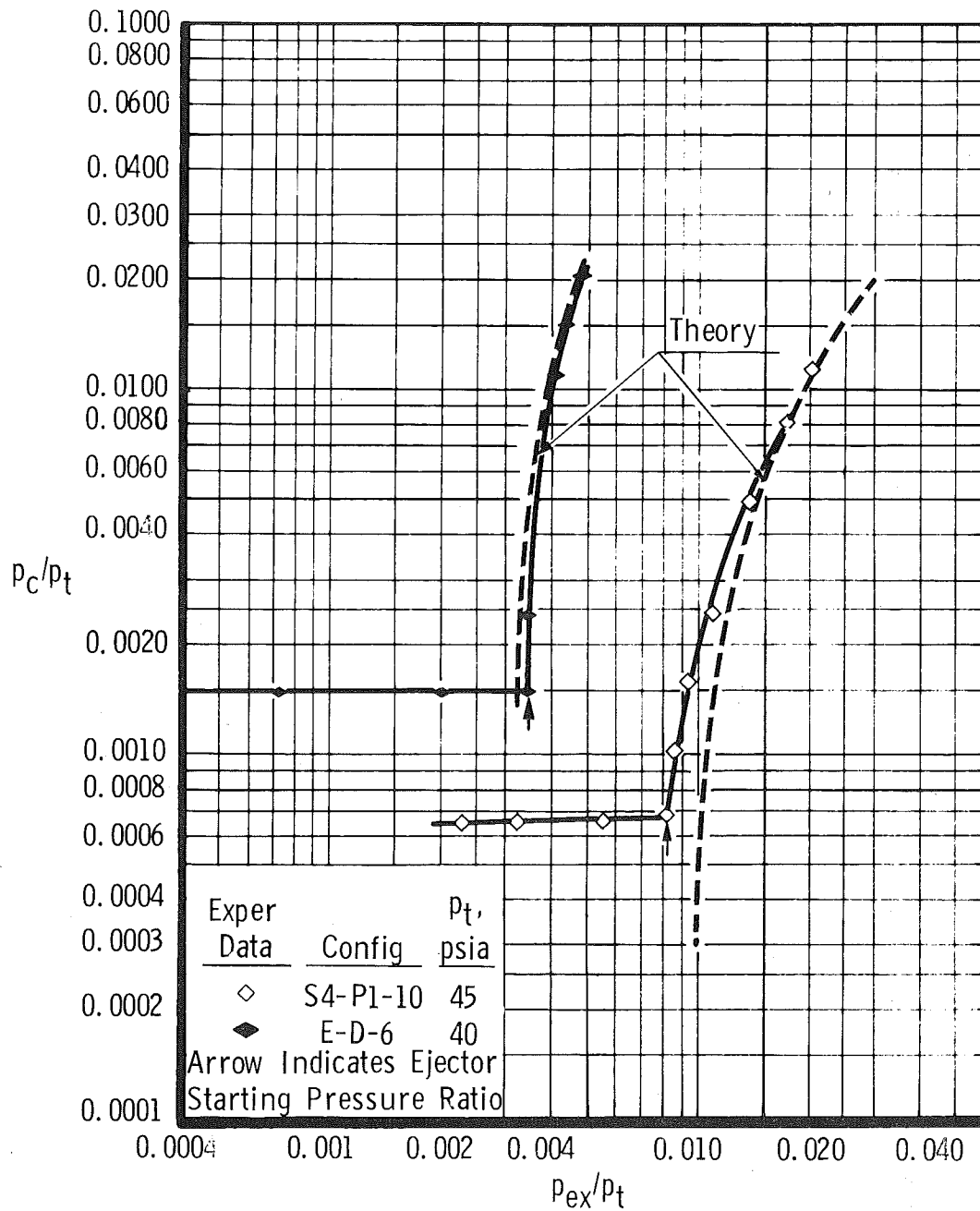


Fig. 13 Graphical Solution for Subsonic Mach Number at Station Two



a. Configurations S1-P2-10, S1-P3-10, S2-P2-10, S3-P1-10, S3-P1-6

Fig. 14 Comparison of Theoretical and Experimental Ejector Pumping Characteristics for Various Annular Nozzle Configurations; $(L/D)_d = 9.0$, $p_t = 45$ psia



b. Configurations S4-P1-10 and E-D-6

Fig. 14 Concluded

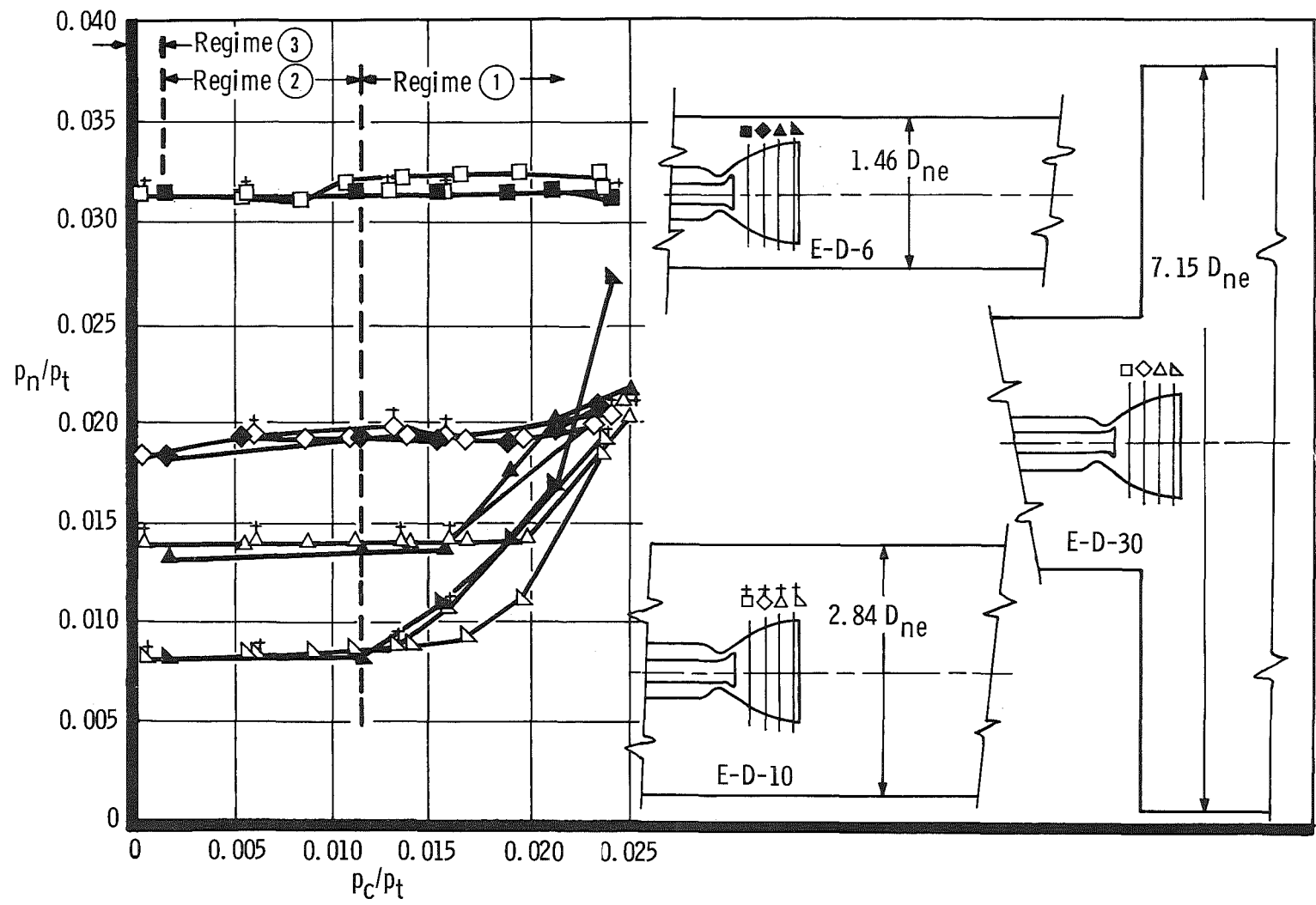


Fig. 15 Effect of Diffuser Diameter on E-D Nozzle Wall Static Pressure Distribution

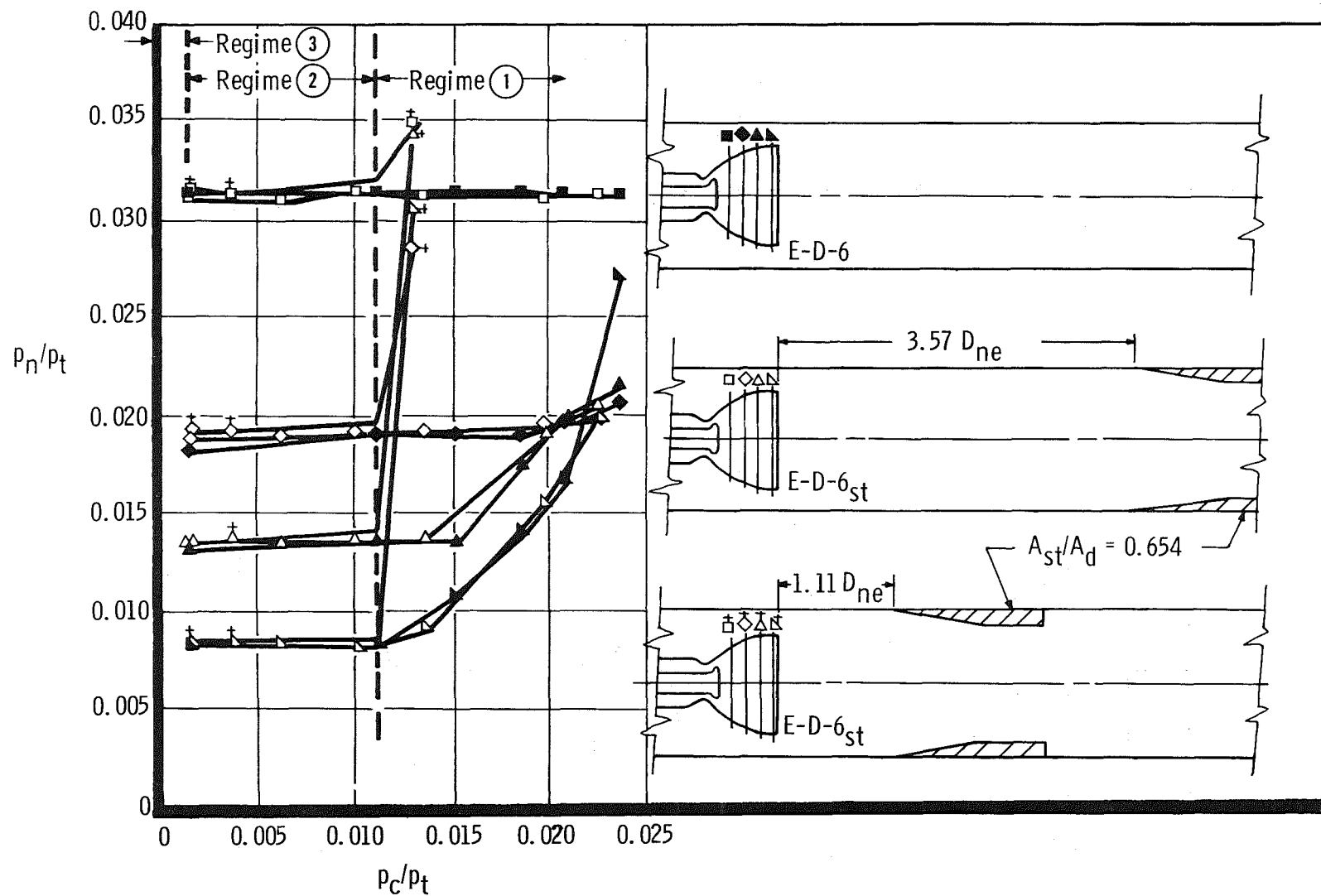


Fig. 16 Effect of Second Throat on E-D Nozzle Wall Static Pressure Distribution, $D_d = 6.12$ in.

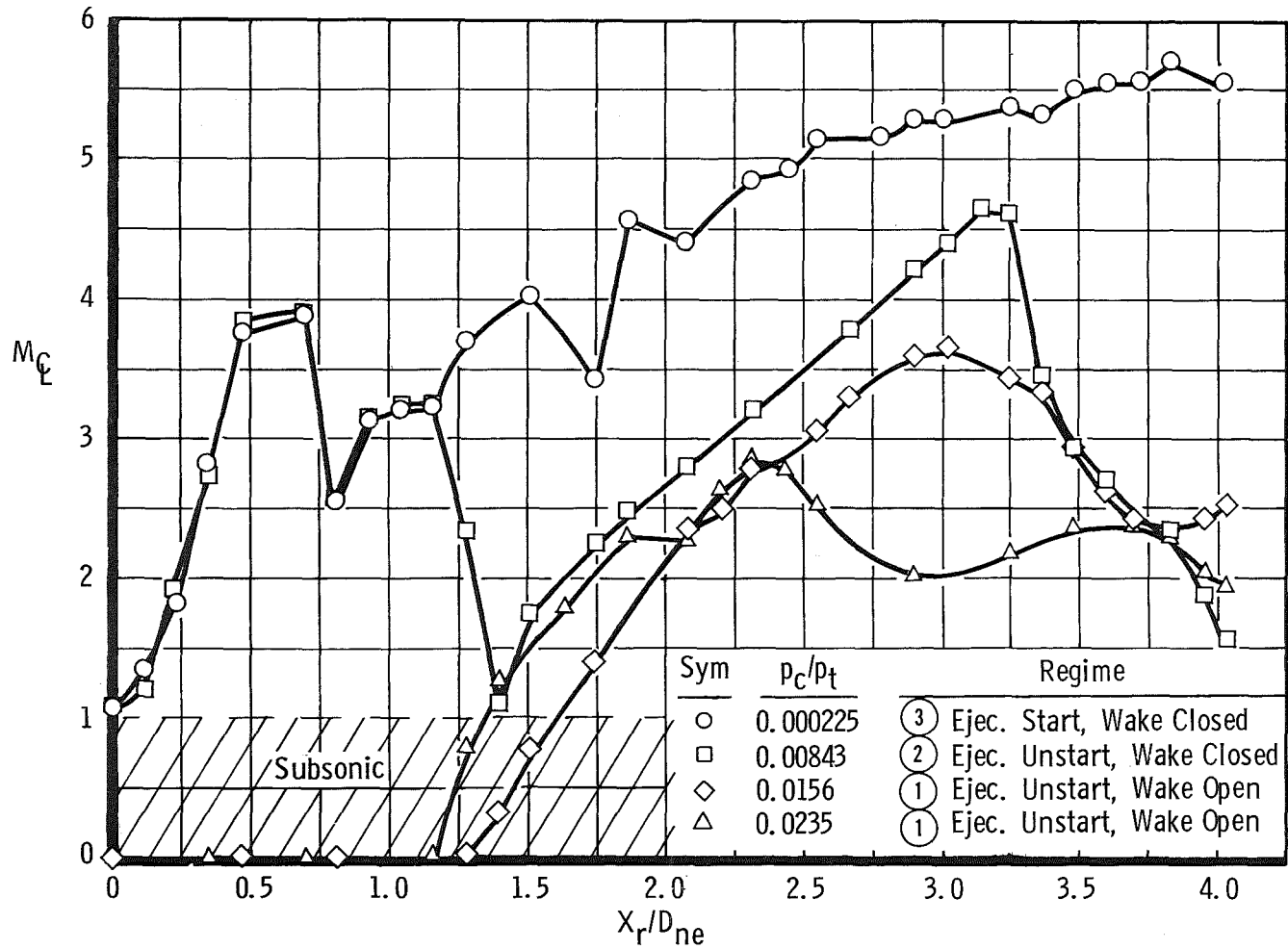


Fig. 17 Mach Number Distribution Downstream of E-D Nozzle for Various Cell Pressure Ratios
($D_d = 10.19$ in., $p_t = 40$ psia)